Available online at www.sciencedirect.com
SCIENCE DIRECT®
International Journal of Thermal Sciences 44 (2005) 89–94
International Journal of Thermal Sciences
www.elsevier.com/locate/ijts

Power optimization of an endoreversible closed intercooled regenerated Brayton cycle

Wenhua Wang [a], Lingen Chen [a,*], Fengrui Sun [a], Chih Wu [b]

[a] *Faculty 306, Naval University of Engineering, Wuhan 430033, PR China*
[b] *Mechanical Engineering Department, US Naval Academy, Annapolis, MD 21402, USA*

Received 10 October 2002; received in revised form 10 June 2003; accepted 21 April 2004

Available online 15 July 2004

Abstract

In this paper, power is optimized for an endoreversible closed intercooled regenerated Brayton cycle coupled to constant-temperature heat reservoirs in the viewpoint of finite-time thermodynamics (FTT) or entropy generation minimization (EGM). The effects of some design parameters, including the cycle heat reservoir temperature ratio and total heat exchanger inventory, on the maximum power and the corresponding efficiency are analyzed by numerical examples. The analysis shows that the cycle dimensionless power can be optimized by searching the optimum heat conductance distributions among the hot- and cold-side heat exchangers, the regenerator and the intercooler for fixed total heat exchanger inventory, and by searching the optimum intercooling pressure ratio. When the optimization is performed with respect to the total pressure ratio of the cycle, the maximum dimensionless power can be maximized again.

Keywords: Finite-time thermodynamics; Brayton cycle; Intercooled; Regenerated; Power; Optimization

1. Introduction

Since the theory of finite-time thermodynamics (FTT) or entropy generation minimization (EGM) was advanced [1–3], much work has been performed for the performance analysis and optimization of finite-time process and finite-size devices [4–10]. Many achievements also have been acquired on the performance analysis of Brayton cycles using FTT [11]. Bejan [12] showed that the power is maximized when the total heat exchanger inventory of an endoreversible simple Brayton cycle is distributed equally between the two heat exchangers. Wu [13,14] analyzed the performance of simple closed Brayton cycles using the method recommended by Curzon and Ahlborn [3] and obtained the numerical result of the maximum power by optimizing cycle power. Cheng and Chen [15] optimized the power of a simple closed irreversible Brayton cycle and analyzed the effects of heat leak, the irreversibility in the compressor and the turbine and the heat conductance distributions between the hot- and cold-side heat exchangers on the maximum power and the corresponding efficiency. Feidt [16] optimized the performance of an irreversible closed regenerated Brayton cycle by taking account of heat resistance and heat leak. Roco et al. [17] found the numerical result of the maximum power and the corresponding efficiency, the maximum efficiency and the corresponding power of an irreversible regenerated Brayton cycle based on Ref. [18]. Sahin et al. [19, 20] optimized the power density of simple and regenerated-reheated Brayton cycle free of heat resistance. Chen et al. [21–24] optimized the distribution of the heat exchanger inventory for maximum power density of the simple and regenerated Brayton cycles with heat resistance and/or other irreversibility. Cheng and Chen [25] built a model for endoreversible intercooled Brayton cycle, evaluated the maximum power and the corresponding efficiency by optimizing the total temperature ratio of the turbine (which is similar to the total pressure ratio) and the temperature ratio of the low-pressure compressor (which is similar to the intercooling pressure ratio) adopting the method recommended in Ref. [26].

* Corresponding author.
E-mail addresses: lgchenna@public.wh.hb.cn, lingenchen@hotmail.com (L. Chen).

1290-0729/$ – see front matter
doi:10.1016/j.ijthermalsci.2004.06.002

Nomenclature

C	thermal capacity rate ..... kW·K^{-1}
E	effectivenesses of heat exchangers
k	specific heats ratio
N	number of heat transfer units
p	pressure..... MPa
P	power ..... kW
$\overline{P}_{\max}$	maximum dimensionless power of the cycle
$(\overline{P}_{\max})_{\max}$	double maximum dimensionless power of the cycle
Q	The rate at which heat is transferred..... kJ
T	temperatures of the working fluid ..... K
U	heat conductances..... kW·K^{-1}
u	heat conductance distribution
π	total pressure ratio
π_1	intercooling pressure ratio
η	efficiency
τ_1	cycle heat reservoir temperature ratio
τ_2	cooling fluid in the intercooler and the cold-side heat reservoir temperature ratio

Superscript

$-$	dimensionless

Subscripts

H, h	hot-side heat exchanger
I, i	intercooler
L, l	cold-side heat exchanger
max	maximum
opt	optimum
$\overline{P}_{\max}$	maximum dimensionless power of the cycle
$(\overline{P}_{\max})_{\max}$	double maximum dimensionless power of the cycle
R, r	regenerator
T	total
wf	working fluid
1, 2, 3, 4, 5, 6, 7, 8	state points

The further step of this paper is to optimize the power of an endoreversible closed intercooled regenerated Brayton cycle coupled to constant-temperature heat reservoirs using FTT by searching the optimum heat conductance distributions among the hot- and cold-side heat exchangers, the regenerator and the intercooler for fixed total heat exchanger inventory, and searching the optimum intercooling pressure ratio and the optimum total pressure ratio. The effects of some design parameters, including the cycle heat reservoir temperature ratio, the cooling fluid in the intercooler and the cold-side heat reservoir temperature ratio and the total heat exchanger inventory, on the maximum power and the corresponding efficiency are analyzed.

2. Theoretical model

Consider an endoreversible intercooled regenerated closed Brayton cycle 1–2–3–4–5–6–1 as shown in Fig. 1. Processes 1–2 and 3–4 are isentropic adiabatic compression in the low- and high-pressure compressors, respectively, while the process 5–6 is isentropic expansion process in the turbine. Process 2–3 is an isobaric intercooling process in the intercooler. Process 4–7 is an isobaric absorbed heat process in the regenerator and process 6–8 is an isobar evolved heat process in the regenerator. Process 7–5 is an isobaric absorbed heat process in the hot-side heat exchanger and process 8–1 an isobar evolved heat process in the cold-side heat exchanger.

Assuming the working fluid used in the cycle is an ideal gas and heat exchangers between the working fluid and the heat reservoirs, the regenerator and the intercooler are counter-flow. According to the properties of working fluid,

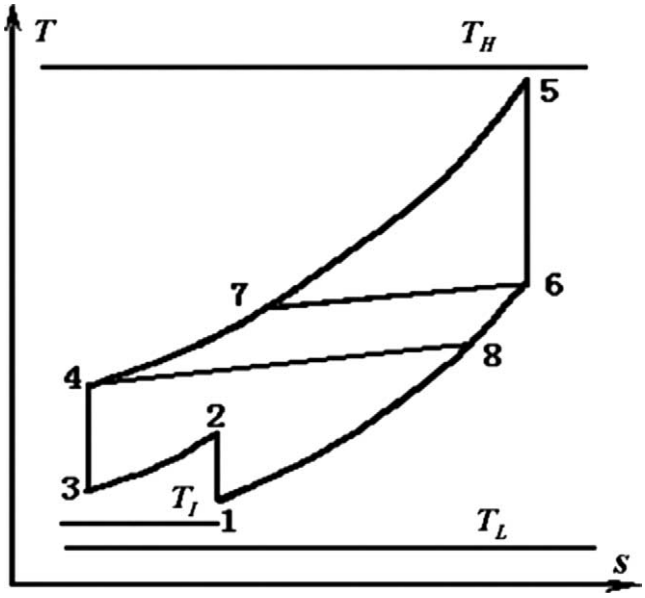

Fig. 1. T–s diagram of an endoreversible intercooled regenerated Brayton cycle.

the heat transfer processes and the theory of heat exchangers, the rate (Q_H) at which heat is transferred from heat source to working fluid, the rate (Q_L) at which heat is rejected from the working fluid to the heat sink, the rate (Q_R) of heat regenerated in the regenerator and the rate (Q_I) of the heat exchanged in the intercooler are, respectively, given by:

$$\begin{aligned} Q_H &= C_{\mathrm{wf}}(T_5 - T_7) \\ &= U_H(T_5 - T_7)/\ln\big[(T_H - T_7)/(T_H - T_5)\big] \\ &= C_{\mathrm{wf}}E_H(T_H - T_7) \end{aligned} \tag{1}$$

$$Q_L = C_{\mathrm{wf}}(T_8 - T_1) = U_L(T_8 - T_1)/\ln\left[(T_8 - T_L)/(T_1 - T_L)\right] = C_{\mathrm{wf}}E_L(T_8 - T_L) \quad (2)$$

$$Q_R = C_{\mathrm{wf}}(T_6 - T_8) = C_{\mathrm{wf}}(T_7 - T_4) = C_{\mathrm{wf}}E_R(T_6 - T_4) \quad (3)$$

$$Q_I = C_{\mathrm{wf}}(T_2 - T_3) = U_I(T_3 - T_2)/\ln\left[(T_3 - T_I)/(T_2 - T_I)\right] = C_{\mathrm{wf}}E_I(T_2 - T_I) \quad (4)$$

where C_{wf} is the thermal capacity rate of the working fluid; U_H, U_L, U_R and U_I are the heat conductances of the hot- and cold-side heat exchangers, the regenerator and the intercooler, respectively; E_H, E_L, E_R and E_I are effectivenesses of the hot- and cold-side heat exchangers, the regenerator and the intercooler, respectively, and are defined as:

$$E_H = 1 - \exp(-N_H), \qquad E_L = 1 - \exp(-N_L)$$
$$E_R = N_R/(N_R + 1), \qquad E_I = 1 - \exp(-N_I) \quad (5)$$

where N_H, N_L, N_R and N_I are numbers of heat transfer units of hot- and cold-side heat exchangers, the regenerator and the intercooler, respectively, and are defined as:

$$N_H = U_H/C_{\mathrm{wf}}, \qquad N_L = U_L/C_{\mathrm{wf}}$$
$$N_R = U_R/C_{\mathrm{wf}}, \qquad N_I = U_I/C_{\mathrm{wf}} \quad (6)$$

The cycle power output and the efficiency are:

$$P = Q_H - Q_L - Q_I = C_{\mathrm{wf}}(T_1 - T_2 + T_3 + T_5 - T_7 - T_8) \quad (7)$$

$$\eta = P/Q = 1 - (T_8 - T_1 + T_2 - T_3)/(T_5 - T_7) \quad (8)$$

Defining the dimensionless power $\overline{P} = P/(C_{\mathrm{wf}}T_L)$, one has:

$$\begin{aligned}\overline{P} = {} & \Big[\big\{(1-E_L)(1-E_I)E_R\pi^{2m} \\ & + \big[(1-E_L)(1-2E_R)(1-E_I) - 1\big]\pi^m \\ & - (1-E_L)(1-E_R)\big(1-E_I\pi_1^m\big) + 1\big\}E_H\tau_1 \\ & + \big\{\big[(1-E_R)E_H + E_R\big](1-E_I)\pi^{2m} \\ & + \big[(1-E_H)(1-2E_R)(1-E_I) - \big(1-E_I\pi_1^m\big)\big]\pi^m \\ & + (1-E_H)\big(1-E_I\pi_1^m\big)E_R\big\}E_L \\ & + \big\{\big[(1-E_L)E_R + (1-E_R)E_H\pi_1^{-m} \\ & + E_LE_R\pi_1^{-m}\big]\pi^{2m} \\ & + \big[(1-E_H)(1-2E_R)\big(1+E_L\pi_1^{-m} - E_L\big) - 1\big]\pi^m \\ & + (1-E_H)E_R\big\}E_I\tau_2\Big] \\ & \times \Big[(1-E_L)(1-E_I)E_R\pi^{2m} \\ & + \big[(1-E_H)(1-E_L)(1-2E_R)(1-E_I) - 1\big]\pi^m \\ & + (1-E_H)E_R\Big]^{-1}\end{aligned} \quad (9)$$

$$\begin{aligned}\eta = {} & 1 - \Big[\big[(1-E_L)\big(1-\pi_1^mE_I\big) - 1\big](1-E_R)E_H\tau_1 \\ & - \big\{(1-E_I)E_R\pi^{2m} \\ & + \pi^m\big[(1-E_H)(1-2E_R)(1-E_I) - \big(1-\pi_1^mE_I\big)\big] \\ & + (1-E_H)\big(1-\pi_1^mE_I\big)E_R\big\}E_L \\ & - \big\{\pi^{2m}\big(1-E_L+\pi_1^{-m}E_L\big)E_R \\ & + \pi^m\big[(1-E_H)(1-2E_R)\big(1-E_L+\pi_1^{-m}E_L\big) - 1\big] \\ & + (1-E_H)E_R\big\}E_I\tau_2\Big] \\ & \times \Big[\big\{(1-E_L)(1-E_I)E_R\pi^{2m} \\ & + \pi^m\big[(1-E_L)(1-2E_R)(1-E_I) - 1\big] + E_R\big\}E_H\tau_1 \\ & + (1-E_R)(1-E_I)E_HE_L\pi^{2m} \\ & + (1-E_R)E_HE_I\pi^{2m}\pi_1^{-m}\tau_2\Big]^{-1}\end{aligned} \quad (10)$$

where $\pi_1 = p_2/p_1$ is the intercooling pressure ratio (pressure ratio of the low pressure compressor), $\pi = p_4/p_1$ is the total pressure ratio of the low and high pressure compressor, $\tau_1 = T_H/T_L$ is total pressure ratio, $\tau_2 = T_I/T_L$ is cooling fluid in the intercooler and the cold-side heat reservoir temperature ratio, and $m = (k-1)/k$ (k is specific heats ratio).

If the regenerated and intercooling processes are not involved in the cycle ($E_R = 0$, $\pi_1 = 1$ and $E_I = 0$), the cycle becomes an endoreversible simple Joul–Brayton cycle. Then, Eqs. (9) and (10) become

$$\overline{P} = \frac{E_HE_L}{(E_HE_L - E_H - E_L)} \times \left[\left(\pi^{-m} - 1\right)\tau_1 + \left(\pi^m - 1\right)\right] \quad (11)$$

$$\eta = 1 - \frac{\pi^m - \tau_1}{\pi^{2m} - \pi^m\tau_1} \quad (12)$$

$\overline{P}$ can be maximized with respect to the total pressure ratio by taking

$$\partial\overline{P}/\partial\pi = 0 \quad (13)$$

and solving for the optimum π. The result is

$$\pi = \tau_1^{1/(2m)} \quad (14)$$

Substituting Eq. (14) into Eq. (12) yields

$$\eta = 1 - \sqrt{1/\tau_1} = 1 - \sqrt{T_L/T_H} \quad (15)$$

Eq. (15) is the same as the Noikov–Chambadal–Curzon–Ahlborn efficiency [1–3].

3. Power optimization

Eqs. (5), (6) and (9) indicate that the cycle dimensionless power $\overline{P}$ is the function of total pressure ratio (π), intercooling pressure ratio (π_1), cycle heat reservoir temperature ratio (τ_1), cooling fluid in the intercooler and the cold-side heat reservoir temperature ratio (τ_2), heat conductance of hot-side heat exchanger (U_H), heat conductance of cold-side heat exchanger (U_L), heat conductance of regenerator (U_R) and heat conductance of intercooler (U_I). For the fixed

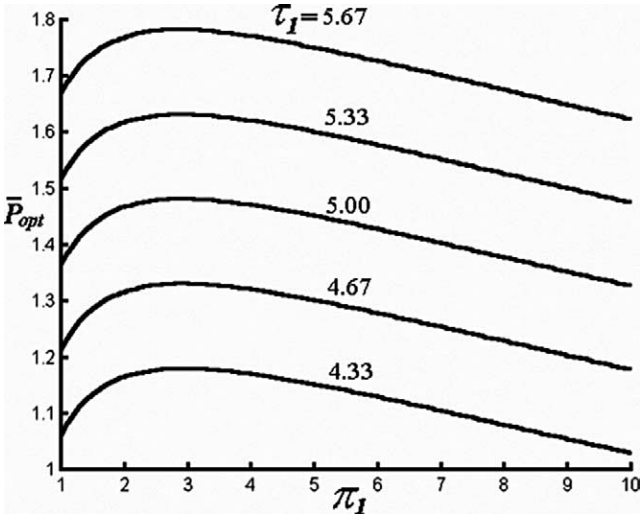

Fig. 2. Optimal dimensionless power versus heat reservoir temperature ratio and intercooling pressure ratio ($U_T = 5$ kW·K^{-1}, $\pi = 10$).

π and π_1, there exist a group of optimal distributions among U_H, U_L, U_R and U_I which lead to the optimal dimensionless power ($\overline{P}_{\text{opt}}$) as the total heat exchanger inventory (U_T, and $U_T = U_H + U_L + U_R + U_I$) is fixed. For the fixed π, there exist a group of optimal distributions among U_H, U_L, U_R and U_I as U_T is fixed and an optimal intercooling pressure ratio which lead to the maximum dimensionless power ($\overline{P}_{\max}$). If π, π_1, U_H, U_L, U_R and U_I all are changeable, there exist a group of optimal distributions among U_H, U_L, U_R and U_I for the fixed U_T and a pair of optimal total pressure ratio and optimal intercooling pressure ratio which lead to the double maximum dimensionless power ($(\overline{P}_{\max})_{\max}$).

For the fixed total heat exchange inventory ($U_T = U_H + U_L + U_R + U_I$), defining:

$$u_h = U_H/U_T, \qquad u_l = U_L/U_T$$
$$u_i = U_I/U_T, \qquad u_r = 1 - u_h - u_l - u_i \tag{16}$$

leads to:

$$U_H = u_h U_T, \qquad U_L = u_l U_T$$
$$U_I = u_i U_T, \qquad U_R = (1 - u_h - u_l - u_i) U_T \tag{17}$$

Additionally, one has the constraints:

$$0 < u_h + u_l < 1, \qquad 0 < u_h + u_i < 1$$
$$0 < u_l + u_i < 1, \qquad 0 < u_h + u_l + u_i < 1 \tag{18}$$

The power optimization is performed by numerical calculations, and the computational program is integrated with the optimization toolbox [27]. In the calculations, $k = 1.4$, $\tau_2 = 1$ and $C_{\text{wf}} = 1.0$ kW·K^{-1} are set.

Fig. 2 shows the characteristic of $\overline{P}_{\text{opt}}$ versus π_1 and τ_1 with $U_T = 5.0$ kW·K^{-1} and $\pi = 10$. The curves are parabolic-like ones. $\overline{P}_{\text{opt}}$ increases with the increase in τ_1. It indicates that there exists an optimal intercooling pressure ratio ($(\pi_1)_{\overline{P}_{\max}}$) that leads to $\overline{P}_{\max}$ (the climax of each curve).

The effect of τ_1 on the characteristic of $\overline{P}_{\max}$ and efficiency ($\eta_{\overline{P}_{\max}}$) corresponding to the maximum dimensionless power versus π with $U_T = 5.0$ kW·K^{-1} is shown in

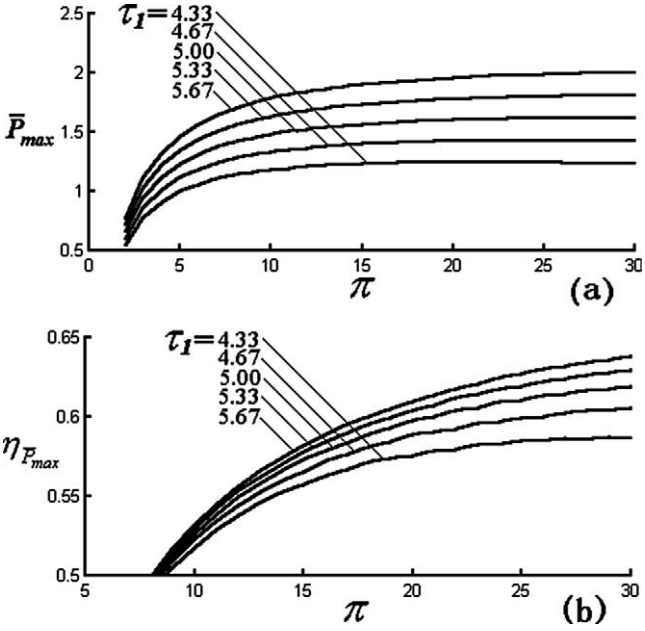

Fig. 3. (a) Maximum dimensionless power versus heat reservoir temperature ratio and total pressure ratio ($U_T = 5$ kW·K^{-1}); (b) Efficiency corresponding to maximum dimensionless power versus heat reservoir temperature ratio and total pressure ratio ($U_T = 5$ kW·K^{-1}).

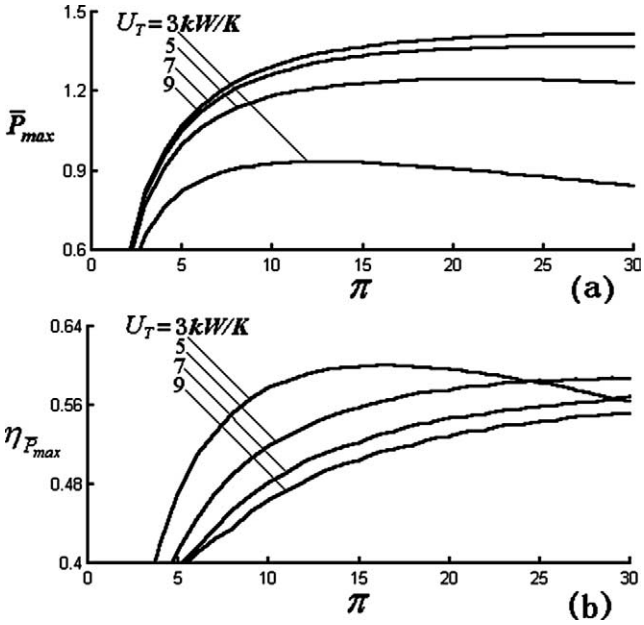

Fig. 4. (a) Maximum dimensionless power versus total heat exchanger inventory and total pressure ratio ($\tau_1 = 4.33$); (b) Efficiency corresponding to maximum dimensionless power versus total heat exchanger inventory and total pressure ratio ($\tau_1 = 4.33$).

Fig. 3(a) and (b), respectively. The effect of U_T on $\overline{P}_{\max}$ and $\eta_{\overline{P}_{\max}}$ versus π with $\tau_1 = 4.33$ is shown in Fig. 4(a) and (b), respectively.

Fig. 3(a) indicates that $\overline{P}_{\max}$ increases to its maximum ($(\overline{P}_{\max})_{\max}$, also the double maximum dimensionless power) rapidly then decreases slowly as π increases. The increase in τ_1 can make $\overline{P}_{\max}$ and $(\overline{P}_{\max})_{\max}$ increase. Fig. 3(b) shows

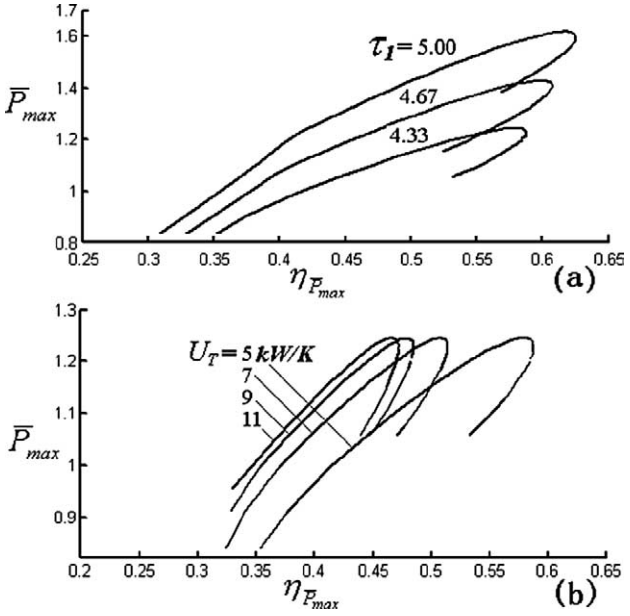

Fig. 5. (a) Maximum dimensionless power versus efficiency corresponding to the maximum dimensionless power and cycle heat reservoir temperature ratio ($U_T = 5$ kW·K^{-1}, $2 < \pi < 80$); (b) Maximum dimensionless power versus efficiency corresponding to the maximum dimensionless power and total heat exchanger inventory ($\tau_1 = 4.33$, $2 < \pi < 80$).

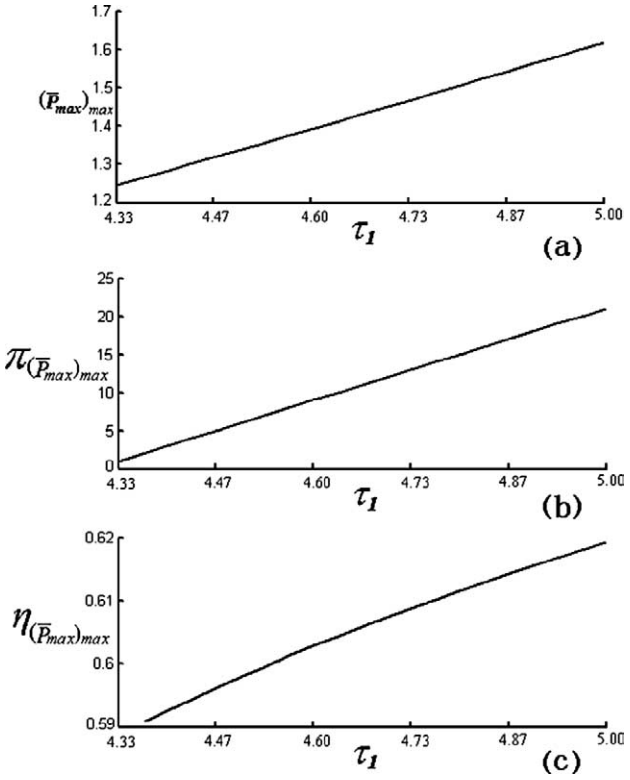

Fig. 6. (a) Double maximum dimensionless power versus cycle heat reservoir temperature ratio ($U_T = 5$ kW·K^{-1}, $2 < \pi < 30$); (b) Total pressure ratio corresponding to double maximum dimensionless power versus cycle heat reservoir temperature ratio ($U_T = 5$ kW·K^{-1}, $2 < \pi < 30$); (c) Efficiency corresponding to double maximum dimensionless power versus cycle heat reservoir temperature ratio ($U_T = 5$ kW·K^{-1}, $2 < \pi < 30$).

that $\eta_{\overline{P}_{max}}$ increases with the increase in τ_1 and π. If π free to increase, $\eta_{\overline{P}_{max}}$ will exhibit a maximum with respect to π.

From Fig. 4(a), one can find that the characteristic curves of $\overline{P}_{max}$ versus π are parabolic-like ones. As π increases, $\overline{P}_{max}$ increases to the double maximum ($(\overline{P}_{max})_{max}$, viz. the climax of each curve) rapidly, and then decreases smoothly. As U_T increases, $\overline{P}_{max}$ increases. When U_T is larger than one value, the increment of $\overline{P}_{max}$ is less and less. Fig. 4(b) shows that $\eta_{\overline{P}_{max}}$ is a parabolic-like function of π. For fixed π, $\eta_{\overline{P}_{max}}$ is a decreasing function of U_T.

Fig. 5(a) and (b) show the effects of τ_1 and U_T on the characteristic of $\overline{P}_{max}$ versus $\eta_{\overline{P}_{max}}$ with $U_T = 5$ kW·K^{-1}, $2 < \pi < 80$ and $\tau_1 = 4.33$, $2 < \pi < 80$, respectively.

The characteristic of $(\overline{P}_{max})_{max}$ versus τ_1 is shown in Fig. 6(a). The corresponding optimal total pressure ratio ($\pi_{(\overline{P}_{max})_{max}}$) and the corresponding efficiency ($\eta_{(P_{max})_{max}}$) versus τ_1 are shown in Fig. 6(b) and (c), respectively. Fig. 6 indicates that $(\overline{P}_{max})_{max}$, $\pi_{(\overline{P}_{max})_{max}}$ and $\eta_{(P_{max})_{max}}$ increase as τ_1 increases.

The characteristic of $(\overline{P}_{max})_{max}$ versus U_T is shown in Fig. 7(a). The corresponding optimal total pressure ratio

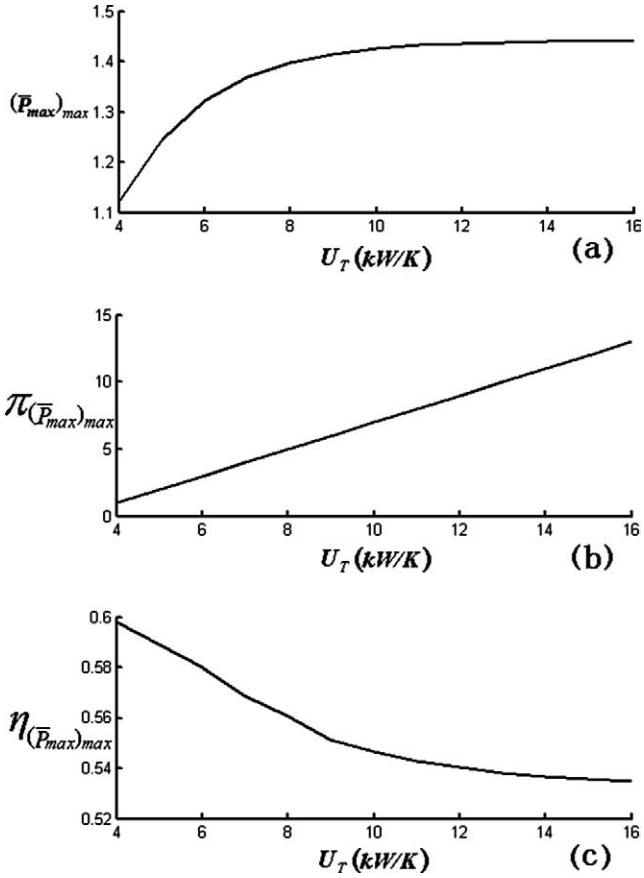

Fig. 7. (a) Double maximum dimensionless power versus cycle heat reservoir temperature ratio ($\tau_1 = 4.33$, $2 < \pi < 30$); (b) Total pressure ratio corresponding to double maximum dimensionless power versus cycle heat reservoir temperature ratio ($\tau_1 = 4.33$, $2 < \pi < 30$); (c) Efficiency corresponding to double maximum dimensionless power versus cycle heat reservoir temperature ratio ($\tau_1 = 4.33$, $2 < \pi < 30$).

($\pi_{(\overline{P}_{\max})_{\max}}$) and the corresponding efficiency ($\eta_{(P_{\max})_{\max}}$) versus U_T are shown in Fig. 7(b) and (c), respectively. As U_T increases, $(\overline{P}_{\max})_{\max}$ and $\pi_{(\overline{P}_{\max})_{\max}}$ increase too, but the increment of the double maximum dimensionless power is less and less. $\eta_{(P_{\max})_{\max}}$ decreases with increase in U_T.

4. Conclusion

Finite-time thermodynamics is applied to optimize the power of an endoreversible closed intercooled regenerated Brayton cycle in this paper. The analysis indicates that there exist a group of optimal values in π_1, U_H, U_L, U_R and U_I which lead to maximum dimensionless power, and there exists an optimal total pressure ratio of the cycle which leads to a double maximum power output. The maximum power increases with the increases in the cycle heat reservoir temperature ratio and the total heat exchanger inventory. The cycle power ($\overline{P}_{\max}$ or $(\overline{P}_{\max})_{\max}$) output increases with the increase in the total heat exchanger inventory (U_T). When U_T is larger than a particular value, the increment of the cycle power is less and less. Additionally, the efficiency ($\eta_{\overline{P}_{\max}}$ or $\eta_{(P_{\max})_{\max}}$) corresponding to maximum or double maximum power decreases with the increase in U_T. The total pressure ratio corresponding to the double maximum power increases with the increases in the cycle heat reservoir temperature ratio and the total heat exchanger inventory. The analysis and optimization presented herein may provide guidelines for power optimization design for the closed gas turbine power plants.

Acknowledgements

This paper is supported by The Foundation for the Author of National Excellent Doctoral Dissertation of PR China (Project No. 200136) and The National Key Basic Research and Development Program of P.R. China (Project No. G2000026301).

References

[1] I.I. Novikov, The efficiency of atomic power stations (A review), Atom. Energ. 3 (11) (1957) 409.
[2] P. Chambadal, Les Centrales Nuclearies, Armand Colin, Paris, 1957, pp. 41–58.
[3] F.L. Curzon, B. Ahlborn, Efficiency of a Carnot engine at maximum power output, Amer. J. Phys. 43 (1) (1975) 22–24.
[4] B. Andresen, Finite-Time Thermodynamics, Physics Laboratory II, University of Copenhagen, Copenhagen, 1983.
[5] A. De Vos, Endoreversible Thermodynamics of Solar Energy Conversion, Oxford University Press, Oxford, 1992.
[6] A. Bejan, Entropy generation minimization: the new thermodynamics of finite-size devices and finite-time processes, J. Appl. Phys. 79 (3) (1996) 1191–1218.
[7] L. Chen, C. Wu, F. Sun, Finite time thermodynamic optimization of entropy generation minimization of energy systems, J. Non-Equilib. Thermodyn. 24 (4) (1999) 327–359.
[8] R.S. Berry, V.A. Kazakov, S. Sieniutycz, Z. Szwast, A.M. Tsirlin, Thermodynamic Optimization of Finite Time Process, Wiley, Chichester, 1999, p. 471.
[9] S. Sieniutycz, A. De Vos (Eds.), Thermodynamics of Energy Conversion and Transport, Springer, New York, 2000, p. 335.
[10] C. Wu, L. Chen, J. Chen (Eds.), Recent Advances in Finite Time Thermodynamics, Nova Science, New York, 1999, p. 560.
[11] L. Chen, Y. Wu, F. Sun, Finite time thermodynamic analysis for gas turbine cycle: theory and application, Gas Turbine Technol. 14 (1) (2001) 46–53 (in Chinese).
[12] A. Bejan, Theory of heat transfer-irreversible power plants, Internat. J. Heat Mass Transfer 31 (6) (1988) 1211–1219.
[13] C. Wu, Power Optimization of a finite-time closed gas-turbine power plant, Internat. J Energy Enviroment Economics 2 (1) (1992) 57–62.
[14] C. Wu, Simulation analysis and optimization of a finite-time gas power plant, Internat. J. Power Energy Syst. 13 (3) (1993) 73–77.
[15] C.Y. Cheng, C.K. Chen, Power optimization of an irreversible Brayton heat engine, Energy Sources 19 (5) (1997) 461–474.
[16] M. Feidt, Optimization of d'un cycle de Brayton moteuren contact avec capacities thermiques finies, Rev. Cen Therm. 35 (12) (1996) 662–666.
[17] J.M.M. Roco, S. Veleasco, A. Medina, A. Calvo Hernaudez, Optimum performance of a regenerative Brayton thermal cycle, J. Appl. Phys. 82 (6) (1997) 2735–2741.
[18] L. Chen, N. Ni, G. Cheng, F. Sun, FTT performance of a closed regenerated Brayton cycle coupled to variable-temperature heat reservoirs, in: Proc. Int. Conf. on Marine Engng., Shanghai, 4–8 November 1996, 1996, pp. 3.7.1–3.7.7.
[19] B. Sahin, A. Kodal, T. Yilmaz, H. Yavuz, Maximum power density analysis of an irreversible Joul–Brayton engine, J. Phys. D: Appl. Phys. 29 (11) (1996) 1162–1167.
[20] B. Sahin, A. Kodal, S.S. Kaya, A comparative performance analysis of irreversible regenerative reheating Joul–Brayton engines under maximum power density and maxium power conditions, J. Phys. D: Appl. Phys. 31 (20) (1998) 2125–2131.
[21] L. Chen, J. Zheng, F. Sun, C. Wu, Optimum distribution of heat exchanger inventory for power density optimization of an endoreversible closed Brayton cycle, J. Phys. D: Appl. Phys. 34 (3) (2001) 422–427.
[22] L. Chen, J. Zheng, F. Sun, C. Wu, Power density optimization for an irreversible closed Brayton cycle, Open Systems & Information Dynamics 8 (3) (2001) 241–260.
[23] L. Chen, J. Zheng, F. Sun, C. Wu, Power density optimization for an irreversible regenerated closed Brayton cycle, Phys. Scripta 64 (3) (2001) 184–191.
[24] L. Chen, J. Zheng, F. Sun, C. Wu, Power density analysis and optimization of a regenerated closed variable-temperature heat reservoir Brayton cycle, J. Phys. D: Appl. Phys. 34 (11) (2001) 1727–1739.
[25] C.Y. Cheng, C.K. Chen, Maximum power of an endoreversible intercooled Brayton cycle, Internat. J. Energy Res. 24 (6) (2000) 485–494.
[26] K. Dvid, C. Ward, Numerical Analysis, Pacific Grove, Brooks/Cole, 1991, Chapter 3.
[27] D.C. Hanselmen, Mastering MATLAB: A Comprehensive Tutorial and Reference, Prentice-Hall, Englewood Cliffs, CA, 1996.